Alma Mater Studiorum Università di Bologna
Archivio istituzionale della ricerca

Ranging On-Demand Microwave Power Transfer in Real-Time

(Article begins on next page)

06 October 2024

Ranging On-demand Microwave Power Transfer in Real-time

Abstract— **This paper presents a novel system for real-time ranging the wireless power transfer "on-demand". This is obtained by duty-cycling a frequency diverse array (FDA) and by suitably choosing the time delay of the pulse. First the theoretical design of the time- and frequency- dependent array is developed, then ranging performances are computed for a 16-element linear array. The simulations demonstrate the system ability not only to dynamically select the area for energy focusing, but also to reduce the energy intensity in undesired areas. Obviously, the sharpness of this operation depends on the number of elements of the array. For validation purposes a demonstrator has been implemented making use of a Xilinx RFSoC ZCU111 to dynamically generate various radio signal excitations of the antenna array. To comply with the adopted SDR the operating frequency is 1.8 GHz and a 4-element array is used. First measurements confirm the ranging capabilities of the proposed solution.**

Keywords— **Ranging, wireless power transfer, SDR, active antenna array.**

I. INTRODUCTION

In recent years, many innovative solutions have been proposed to optimize the receiver sides of WPT systems, for both far-field and near-field techniques. However there are still far fewer solutions available for optimizing the transmitter side, in particular for enabling the location and tracking of the devices to be charged. This is a substantial need when the aim is to remotely energize objects that are either in motion or located in different positions in the same environment, such as for power supplying low-power light-weighed Unmanned Aerial Vehicle (UAV) [1].

Although some attempts have been proposed based on advanced inductive power transfer systems (IPT) for short-range purposes [2][3], far-field WPT techniques are more suitable for these application sectors. In particular, focusing technique are exploited and among them frequency diverse arrays (FDA) can be excellent candidates because they enable angle and range focusing capabilities [4].

This work proposes a novel exploitation of microwave WPT techniques adopting a time-based control technique applied to an FDA array to enable reconfigurable power beaming with the capability of modifying the target area in real-time. This is obtained by combining duty cycling of the FDA signal excitations with a suitable time delay, thus obtaining a delayed pulsed FDA. It is demonstrated that by choosing the pulse duration allows to define the target area extension, while the proper time delay sets the focus range.

It is demonstrated that the proposed solution improves the overall WPT system efficiency with the twofold advantage of focusing more energy where it is needed and at the same time of minimizing the wasted energy radiation in those regions where it cannot be exploited.

II. TIME CONTROLLED FREQUENCY DIVERSE ARRAYS

Let us consider a linear array of M elements aligned along the x-axis, with $d_m = d_0 + \Delta d_m$ as the distance of the m-th element from the reference frame origin (here considered coincident with the phase center of the basis (0-th) antenna), as schematically reported in Fig. 1. For standard Frequency Diverse Arrays (FDAs) the following relationships hold:

$$\begin{cases} d_m = m * d_0 \\ f_m = f_0 + \Delta f_m = f_0 + m * \Delta f \end{cases} \qquad (1)$$

where f_0 is the radio-frequency (RF) carrier of the basis element and Δf is the constant frequency offset among the elements.
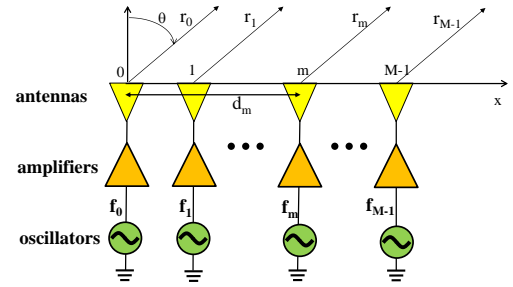

Fig. 1. Scheme of a standard FDA arrangement.

An important limit of FDAs is the time-shifting effect that modifies their radiating properties [4] over time, and needs be removed for WPT purposes by the time-controlled strategy that is proposed in the following. Let us consider (2) as the time-controlled signal transmitted by the m-th element of the array:

$$x_m(t) = \exp(j2\pi f_m t) * x_T(t - \tau) \qquad (2)$$

where $x_T(t - \tau)$ is a delayed rectangular pulse, with a proper duty cycle, modulating the m-th RF input signal, whose Fourier expansion is:

$$x_T(t - \tau) = \sum_{n=0}^{n_h} a_n cos\left(n \frac{2\pi}{T}(t - \tau)\right) \qquad (3)$$

where $a_n = \frac{2A}{n\pi} si n\left(\frac{n\pi T_p}{T}\right), a_0 = \frac{A T_p}{T}$, τ is the key parameter to be chosen in order to delay the pulse within the FDA period in such a way that the time-dependency of the FDA focusing is cancelled, $T = \frac{1}{\Delta f}$, T_p represents the on-duration of the pulse, A is the pulse amplitude, and n_h the number of harmonics of interest (250, for the present case).

Under the hypothesis $f_0 \gg \max(\Delta f_m)$, the array factor (AF) in the far-field region can be cast in the following way [4]:

$$AF(t,\theta,r) = \sum_{m=0}^{M-1} b_m \, exp\left(j2\pi f_0 \left(\frac{d_m \sin(\theta)}{c}\right)\right) *$$
$$exp\left(j2\pi \Delta f_m \left(t - \frac{r_0}{c}\right)\right) * x_T\left(t - \tau - \frac{r_m}{c}\right) \qquad (4)$$

where c is the speed of light and b_m is the complex coefficient of the excitation current feeding the m-th element of the array. As for a traditional phased-array, the proper choice of b_m can provide the desired steering angle of the main lobe. Except when explicitly underlined, $b_m = 1$ in the following, which means broadside radiation.

The novel introduction of the modulating signal $x_T(t - \tau)$ aims at counterbalancing the natural time-dependency of (4) (in the second exponential term). This makes the new radiating system a time-controlled FDA (TCFDA), which allows to control not only the direction but also the range of a specific target (r, θ) area, almost in real-time, and to ensure time-stability of this operation. By properly choosing the two shaping parameters (T_p and τ), fix-in-time focusing of the radiation (therefore the power identified by the beam pattern $(= |AF(t,\theta,r)|^2)$) is achieved. This is foreseen to be an excellent added value for next generation on-demand energy transfer systems for applications such as powering on the move drones, objects and people.

The aforementioned behavior is now demonstrated by numerical simulation. As a representative example, let us compute the AF of a TCFDA with M=16, f_0=1.8 GHz, Δf=5 MHz, $T = \frac{1}{\Delta f}$=200 ns, A=1, T_p=20 ns, $\tau = 0$ s and 80 ns, $d_0 = \frac{\lambda}{2}$. The results are shown in Fig. 2 in terms of the normalized beam pattern (BP) in the broadside direction (θ=0°), as a function of range and time, and are compared with a standard FDA: they show that by varying τ it is possible to sharply control the illumination region. Fig. 2(a) (corresponding to τ=0 s) shows that the illuminated spot is in the range 0÷5 m, while in Fig. 2(b) the spot is moved to the 20÷25 m range by using the same pulse and setting τ= 80 ns. Of course, the focusing area sharpness, strictly depends on the number of the array elements M and can

be thinned by increasing M. For comparison purposes, an FDA beaviour with respect to the range is plotted in Fig. 2(c): it shows the well-known uncontrolled, thus undesired, time-dependency of the BP [4] in this case. This demonstrates the enhanced beam-focusing capabilities of the proposed TCFDA.

A further effective result of the proposed piloting strategy is provided by the 2-D plots reported (in red) in Figs. 3 and 4, showing the TCFDA performance from the receiver side point of view, in terms of the BP multiplied by the isotropic attenuation (A_{iso}) vs. time, for a receiving antenna with unity gain. For comparison purposes, the behaviours of a standard phased array (with the same pulsed excitation conditions and the same number of elements) are superimposed (blue curves).
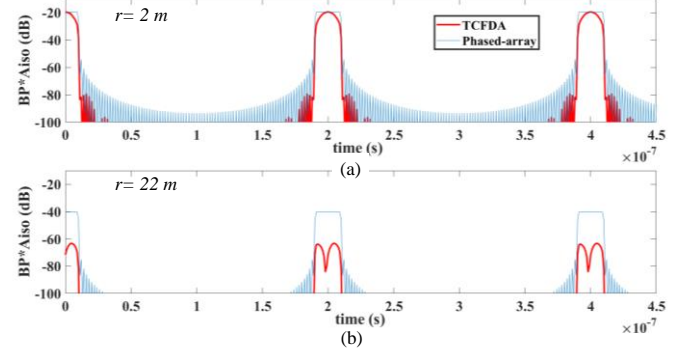
Fig. 3. BP (accounting for isotropic attenuation) vs. time when the TCFDA is designed to focus at (r, θ) =(2m , 0°).
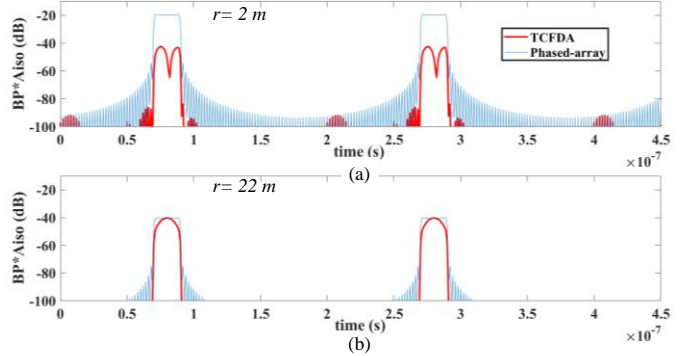
Fig. 4. BP (accounting for isotropic attenuation) vs. time when the TCFDA is designed to focus at (r, θ) =(22 m , 0°).
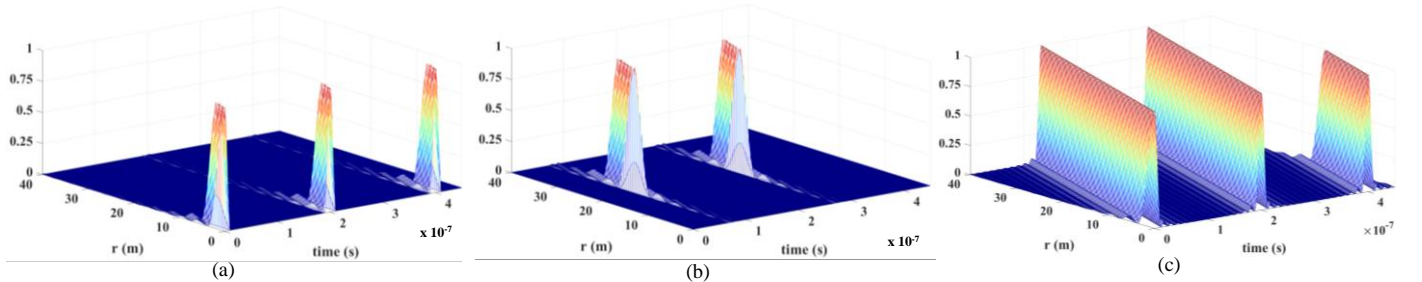
Fig. 2. Normalized beam patterns as a function of range and time with: (a) TCFDA ($T_p = 20\ ns, \tau = 0\ s$); (b) TCFDA ($T_p = 20\ ns, \tau = 80\ ns$); (c) for a standard FDA.

.

These plots show that, by properly choosing the τ parameter, it is possible to concentrate the power source in a specific range and simultaneously put it down in the undesired range, thus enabling dynamic focusing. This is evident in Fig. 3, where by choosing $\tau = 0$ s, the maximum of radiation is obtained in the range $(r, \theta)=(2$ m, $0°)$ (Fig. 3(a)). Fig. 3(b) compares the $BP \cdot A_{iso}$ in the range $(r, \theta)=(22$m, $0°)$ obtained by the proposed system and by a standard phased array: a reduction of about 20 dB is obtained by the TCFDA with respect to the phased array performance in the undesired location. The situation can be dynamically modified, as demonstrated in Figs. 4(a) and (b) where, by selecting $\tau =80$ ns, the target range is moved to $(r, \theta)=(22$m, $0°)$: in such conditions the received signal strength at 22 m is 2-dB higher than in the $(r, \theta)=(2$m, $0°)$, thus overcoming predictions based on Friis formula. In the same figures the pulsed patterns of a phased-array are also superimposed: of course, the latter obeys the Friis formula, thus providing, in the maximum radiation direction, a signal strength diminishing with the squared distance.

III. EXPERIMENTAL SET UP AND RESULTS

A preliminary and, to the authors' knowledge, first proof-of-concept of the TCFDA complex radiating mechanism is presented in this section. The proposed antenna array driving strategy is managed by the Xilinx (RFSoC ZCU111) SDR. The following set up is adopted:

- 4-planar-dipole array resonating at 1.8 GHz;
- RFSoC ZCU111 Evaluation Tool and XM500 RFMC Balun Add-On Card piloting the 4 balanced dipoles;
- Horn receiving antenna TDK RF SOLUTIONS HRN-0110 (connected back to the ZCU111 Board)

Both the choices of the operating frequency and of the array maximum number of elements are imposed by the SDR: the first is a matter of numerical sampling limit, the second is due to the availability of just 4 balanced output ports (the control of additional 8 unbalanced ports would need for the Avnet board AES-LPA 502 G, not yet available in the lab).

The use of a 4-dipole array limits, of course, the focusing potentialities, being the dimension of the spot area around 10 m^2. However, the purpose of this Section is to give the proof-of-concept of the idea previously presented. Because of the limited transmitted power, we measured the received power at a fixed reduced link distance (2 m). Two sets of driving sequences are considered: i) time window $T_p=20$ ns, $\tau=0$ s and 80 ns; ii) time window $T_p=10$ ns, $\tau=0$ s and 75 ns, and the corresponding measured received waveforms are given in Fig. 5 and Fig. 6, respectively, in normalized linear scale.

One can note that T_p and τ play the predicted strategic role in the array focusing design. In fact, the width of the pulse window (T_p) allows to modify the focused area dimension, as can be evinced by comparing Figs. 5 and 6. The pulse position within the FDA period T (τ) selects the maximum (cases (a)) or a minimum (cases (b)) locations.

Because of the office scenario used for measurement, the difference between cases (a) and (b) is worse than the predicted one by simulations (the ratio should be 1/4) probably due to the

real-channel effects (not included in the simulations) . However, this can be considered the first practical proof-of-concept of TCFDA smart beamforming.
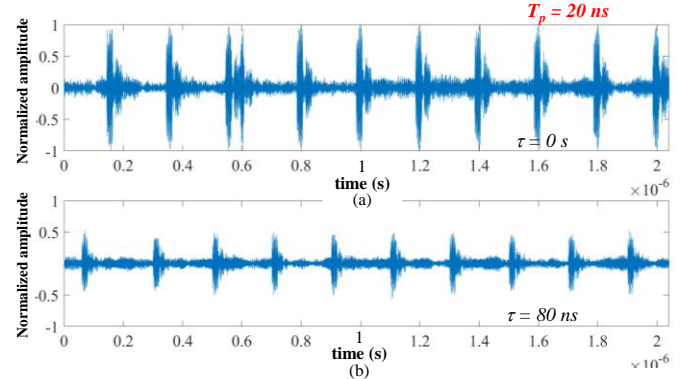

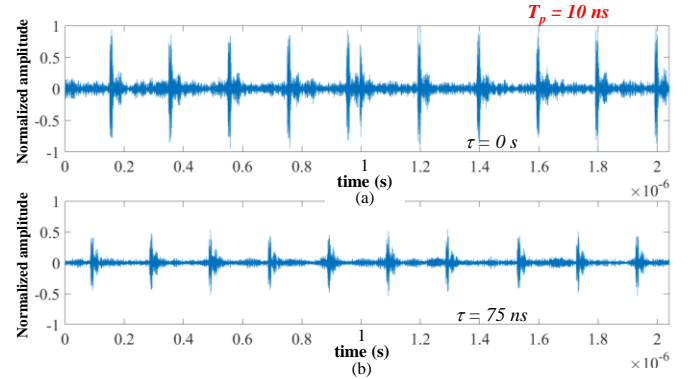Fig. 5. Normalized received signal with $T_p = 20$ n with (a) $\tau = 0$ s; (b) $\tau = 80$ ns .

Fig. 6. Normalized received signal with $T_p = 10$ n with (a) $\tau = 0$ s; (b) $\tau = 75$ ns .

IV. CONCLUSIONS

The time control of the focusing capability of FDA radiating architectures has been theoretically developed and experimentally validated. Pulse width and delay driving the frequency divers array elements excitations are the key parameters for real-time setting the illuminated spot area and range, thus making TCFDA a key player for selective far-field WPT "on-the-move" applications.

REFERENCES

[1] S. Dunbar et al., "Wireless far-field charging of a micro-UAV," 2015 IEEE Wireless Power Transfer Conf., Boulder, CO, 2015, pp. 1-4.
[2] S. Aldhaher, P. D. Mitcheson, J. M. Arteaga, G. Kkelis and D. C. Yates, "Light-weight wireless power transfer for mid-air charging of drones," 11th European Conf. Ant. and Propag., Paris, 2017, pp. 336-340.
[3] J. Bito, S. Jeong and M. M. Tentzeris, "A Novel Heuristic Passive and Active Matching Circuit Design Method for Wireless Power Transfer to Moving Objects," IEEE Trans. Microw. Theory Techn, vol. 65, no. 4, pp. 1094-1102, April 2017.
[4] W. Wang, H. C. So and A. Farina, "An Overview on Time/Frequency Modulated Array Processing," IEEE Journal of Selected Topics in Signal Processing, vol. 11, no. 2, pp. 228-246, March 2017.